Journal of Geophysical Research: Oceans

RESEARCH ARTICLE
10.1029/2018JC014178

Special Section:
The U.S IOOS Coastal and Ocean Modeling Testbed 2013-2017

A Diel Method of Estimating Gross Primary Production: 1. Validation With a Realistic Numerical Model of Chesapeake Bay

Malcolm E. Scully[1]

[1]Applied Ocean Physics and Engineering, Woods Hole Oceanographic Institution, Woods Hole, MA, USA

This article is a companion to Scully (2018), https://doi.org/10.1029/2018JC014179.

Key Points:
- A new method for estimating gross primary production from in situ dissolved oxygen data is presented
- Application of the method to numerical model output demonstrates the method can accurately estimate gross primary production
- Vertical mixing contributes to diurnal oxygen variations, but there is an optimal vertical location where this effect is minimized

Correspondence to:
M. E. Scully,
mscully@whoi.edu

Citation:
Scully, M. E. (2018). A diel method of estimating gross primary production: 1. Validation with a realistic numerical model of Chesapeake Bay. *Journal of Geophysical Research: Oceans*, *123*, 8411–8429. https://doi.org/10.1029/2018JC014178

Received 15 MAY 2018
Accepted 16 OCT 2018
Accepted article online 24 OCT 2018
Published online 25 NOV 2018

©2018. American Geophysical Union. All Rights Reserved.

Abstract A method for estimating gross primary production (GPP) is presented and validated against a numerical model of Chesapeake Bay that includes realistic physical and biological forcing. The method statistically fits a photosynthesis-irradiance response curve using the observed near-surface time rate of change of dissolved oxygen and the incoming solar radiation, yielding estimates of the light-saturated photosynthetic rate and the initial slope of the photosynthesis-irradiance response curve. This allows estimation of GPP with 15-day temporal resolution. The method is applied to the output from a numerical model that has high skill at reproducing both surface and near-bottom dissolved oxygen variations observed in Chesapeake Bay in 2013. The rate of GPP predicted by the numerical model is known, as are the contributions from physical processes, allowing the proposed diel method to be rigorously assessed. At locations throughout the main stem of the Bay, the method accurately extracts the underlying rate of GPP, including pronounced seasonal variability and spatial variability. Errors associated with the method are primarily the result of contributions by the divergence in turbulent oxygen flux, which changes sign over the surface mixed layer. As a result, there is an optimal vertical location with minimal bias where application of the method is most accurate.

Plain Language Summary This paper presents and evaluates a method for estimating gross primary production from time variations of dissolved oxygen. The evaluation is performed on the output from a three-dimensional circulation model of Chesapeake Bay that can simulate dissolved oxygen with high skill.

1. Introduction

For nearly seven decades, researchers have sought to make estimates of primary production from diel changes in dissolved oxygen (DO) concentration in aquatic and marine ecosystems (e.g., Staehr et al., 2012). A specific goal of this line of research has been to quantify the net ecosystem metabolism (NEM). NEM is typically represented as the sum of the gross primary production (GPP) and the community respiration (CR). While GPP represents the autotrophic conversion of inorganic to organic carbon, CR includes the oxidation of organic carbon by both heterotrophic and autotrophic organisms. Although these rates are quantified in terms of production and consumption of carbon, some methods have focused on the fate of oxygen, which is more easily measured with in situ instruments.

The most commonly employed methods for measuring GPP rely on bottle incubations. These techniques are time intensive and not conducive to automated methods using in situ instruments, which often limits their temporal resolution. Additionally, there are a number of known issues with bottle incubation methods (e.g., Marra, 2009). For instance, it is well established that the ^{14}C-CO_2 method can result in underestimates of GPP because some of the introduced ^{14}C is respired during the incubation (Bender et al., 1987; Peterson, 1980). Even short incubations (2–3 hr) can result in underestimates of GPP by an order of magnitude (Cole et al., 1992; Howarth et al., 1996; Milligan et al., 2015). Incubations in bottles eliminate turbulence so that they do not accurately represent the natural light environment (Lewis, 1988; Richey et al., 1990) or the vertical fluxes of nutrients.

In order to avoid these bottle effects, the open-water diel method has been used in a number of environments. This technique, which quantifies diel oxygen variations, has a long history of use (Odum, 1956). The application of this method has primarily been in lakes where weak currents and horizontal gradients limit the influence of horizontal advection (e.g., Staehr & Sand-Jensen, 2007). Changes in oxygen concentration

caused by vertical mixing also must be accounted for. Typically, this is done by assuming that the vertical flux divergence at the measurement location can be quantified from an estimate of the atmospheric gas flux (F_{surf}) divided by the surface mixed-layer depth (z_{mix}; e.g., Cole et al., 2000).

Attempts to employ the diel O_2 approach to measuring GPP in estuaries have illustrated some of the difficulties associated with this approach (Kemp & Boynton, 1980; Howarth et al., 1992; Swaney et al., 1999). Despite some of these difficulties, in situ diel O_2 measurements have a number of advantages over bottle incubations because they sample the natural environment without altering the light, turbulence, or other potentially important natural processes. Improvements in sensor technology have dramatically improved our ability to measure DO in situ. These new sensors enable nearly continuous measurements of DO over deployments lasting many months.

The combination of high-quality continuous DO measurements collected at ocean observatories with open-water diel techniques represents a powerful opportunity to make estimates of GPP with unprecedented temporal resolution. Given the scientific community's increasing reliance on numerical models to study biogeochemical processes, continuous and accurate in situ estimates of GPP could allow a much more rigorous skill assessment of these models against the fundamental biological rates they simulate. Too often, the skill of biogeochemical models is assessed through comparison with DO data (Irby et al., 2016). However, as Scully (2013, 2016a) demonstrates, even a model with no biogeochemical variability can reasonably simulate DO in an estuary that experiences hypoxia because of the dominant role that physical processes play in modulating DO. Thus, a model with high skill at simulating DO may be a very poor representation of the underlying biological dynamics.

In this paper a diel method for estimating GPP from hourly in situ observations of near-surface DO is presented. As detailed below, the method uses a statistical relationship between incoming solar radiation and the time rate of change of DO to estimate GPP. The primary goal of this paper is to assess the accuracy of the method by applying it to the output from a coupled three-dimensional circulation-biogeochemical model that reasonably simulates both biological oxygen production/consumption and physical variations caused by advection and vertical mixing. The formulations for GPP and CR used in the numerical model are derived in a companion analysis (Scully, 2018) of 7 years of hourly near-surface DO data collected through the Chesapeake Bay Interpretive Buoy System. The proposed diel method is applied to the model output of hourly near-surface DO to assess its ability to accurately estimate the rate of GPP used in the model. Unlike previous attempts to evaluate diel techniques, which have relied on simplified models that do not consider the complete three-dimensional contributions of advection and mixing (Cox et al., 2015), the evaluation presented here employs a three-dimensional circulation model with realistic atmospheric, tidal, and riverine forcing. The proposed method is presented in section 2, and the numerical model is described in section 3. A quantitative analysis of the accuracy of the method is present in section 4 and discussed in section 5, and conclusions are presented in section 6.

2. Proposed Diel Method

The diel oxygen technique has been employed since the late 1940s (Sargent & Austin, 1949) and used in a variety of aquatic ecosystems, including Chesapeake Bay (Kemp & Boynton, 1980). The technique is based on the equation for conservation of DO:

$$\frac{\partial O_2}{\partial t} = GPP - CR - u_i \nabla O_2 + \frac{\partial}{\partial z} K_z \frac{\partial O_2}{\partial z} \tag{1}$$

where the time rate of change of DO concentration (term on left-hand side) is controlled by both biological and physical processes. GPP and CR represent the biological sources and sinks, respectively. Gradients in the advective and vertical turbulent fluxes are the third and fourth terms on the right-hand side of equation (1), respectively. Here an eddy diffusivity (K_z) and the down-gradient assumption are used to represent the vertical turbulent flux of oxygen. Equation (1) can be written as

$$\frac{\partial O_2}{\partial t} = GPP + \Delta O_2 \tag{2}$$

where the combined contributions of advection, mixing, and CR are all lumped together in one term (ΔO_2).

Here the convention is that negative values of ΔO_2 decrease $\partial O_2/\partial t$. During the nighttime hours when there is no solar radiation, this simplifies to

$$\frac{\partial \widehat{O}_2}{\partial t} = \Delta \widehat{O}_2 \tag{3}$$

where the hat is used to denote conditions with no incoming light.

In the application of the diel oxygen technique in lakes, the contribution of advection is often assumed to be negligible (Staehr et al., 2010). However, this is not always a good assumption in estuarine environments (Beck et al., 2015; Cox et al., 2015; Howarth et al., 1992; Kemp & Boynton, 1980). In many applications, the contribution of the vertical flux divergence is simply estimated as F_{surf}/z_{mix} (Cole et al., 2000). This approach requires that oxygen is well mixed throughout a surface layer of known depth, assumes that there is no vertical flux at the base of this layer, and requires an accurate estimate of the gas transfer velocity. While methods that deal with the contribution of horizontal advection have been proposed (Howarth et al., 1992; Swaney et al., 1999), these methods require data from multiple stations with appropriate spacing. An alternate method for making estimates of GPP from a single fixed near-surface sensor is proposed below. It is important to note that the method proposed in this paper provides volumetric rates (e.g., $gO_2{\cdot}m^{-3}{\cdot}day^{-1}$) of GPP and assumptions about its vertical distribution must be made in order to convert these estimates to the more commonly reported depth-integrated values (e.g., $gO_2{\cdot}m^{-2}{\cdot}day^{-1}$). Similar assumptions are required when estimating GPP from bottle incubations. Furthermore, the diel method presented here does not provide accurate estimates of CR and hence does not attempt to quantify the NEM.

The method is based upon the fact that the rate of GPP is expected to vary as a function of incoming solar radiation (E). There are numerous proposed formulations for the relationship between primary productivity per unit chlorophyll biomass (P^B) and E (e.g., Jassby & Platt, 1976). While nearly all of the proposed formulations are functionally very similar, Jassby and Platt (1976) found the following relationship to be the most consistently useful mathematical representation of the data:

$$P^B = P^B_m \tanh\left(\frac{\alpha^B E}{P^B_m}\right) \tag{4}$$

where P^B_m is the maximum photosynthetic rate and α^B is the linear slope of the photosynthesis-irradiance response (PE) curve under light-limited conditions. Here the superscript B indicates values that have been normalized by the chlorophyll-a concentration. Directly quantifying the PE curve using diel oxygen variations is complicated by uncertainties in both the photosynthetic quotient (O_2:C; e.g., Laws, 1991) and the chlorophyll-to-carbon ratio (e.g., Cloern et al., 1995). To avoid these uncertainties here, GPP is quantified strictly in terms of oxygen and estimates of the PE curve are not normalized by chlorophyll concentration. Consistent with the traditional notation, we drop the superscript B to denote non-normalized value (e.g., $P_m = mmolO_2{\cdot}m^{-3}{\cdot}s$). With these simplifications, equation (1) can be recast as

$$\frac{\partial O_2}{\partial t} = P_m \tanh\left(\frac{\alpha E}{P_m}\right) + \Delta O_2 \tag{5}$$

where ΔO_2 is simply a constant that represents the contributions from physical transport and biological consumption (e.g., CR). To apply the proposed method, the value of ΔO_2 in equation (5) is estimated by averaging the time rate of change of DO during periods when $E = 0$. This assumes that $\Delta O_2 \sim \Delta \widehat{O}_2$. The observed time rate of change of oxygen is next fit to equation (5) using the estimated value of $\Delta \widehat{O}_2$ and measurements of surface irradiance (E_0) using a two-parameter least squares regression, providing estimates of both P_m and α. This procedure is essentially the same as fitting techniques that provide similar estimates of these parameters from bottle incubations (Gallegos, 2012). In this approach, P_m and α are the only two free parameters with α determining the initial slope of the curve and the ratio P_m/α determining the value of irradiance where light-saturated photosynthesis begins.

The method is applied to 15 days of hourly data. As will be discussed below, this interval is selected to minimize the correlation between tidal processes (primarily semidiurnal) with incoming solar radiation (diurnal). As a result, the parameters of the PE curve are estimated with 15-day temporal resolution. GPP is estimated by

applying the *PE* curve estimates to the hourly estimates of light availability. Thus, even though the temporal resolution of the *PE* curve is 15 days, higher-frequency variability in GPP is predicted due to the hourly variability in irradiance. Temporally averaged values of GPP are calculated from these hourly estimates in order to avoid potential errors associated with nonlinearities with the assumed form of the *PE* curve. Anticipating applying the method to observations where subsurface light data are not available, the method is applied using the surface irradiance, unless otherwise noted. These estimates are compared to similar estimates obtained using the observed subsurface light in section 4.2.

3. Numerical Model Description

A primary goal of this paper is to apply the proposed diel method to the output from a three-dimensional numerical model to assess how well the proposed method can estimate the known rate of GPP that is used in the model. The hydrodynamic model is based on the Chesapeake Bay Regional Ocean Modeling System (ROMS) Community Model (ChesROMS; Xu et al., 2012) and is identical to that used by Scully (2013, 2016a). The forcing for the hydrodynamic model includes realistic tidal and subtidal forcing, observed freshwater inputs, and atmospheric forcing (shortwave solar radiation, longwave radiation, rainfall, surface air humidity, pressure, temperature, and 10-m winds) derived from the North American Regional Reanalysis (NARR) model. The overall approach is to use the simplest model that can adequately capture the dominant processes that modulate DO in Chesapeake Bay. Unlike previous efforts, which have focused on isolating the role of physical processes (e.g., Scully, 2013), here a more realistic approach is used that includes analytical formulations for GPP and CR. These formulations are based on an analysis of high-frequency observational data in order to capture the dominant temporal and spatial variations in oxygen observed in Chesapeake Bay (Scully, 2018).

Consistent with equation (4), GPP is modeled as

$$\mathrm{GPP} = P_\mathrm{m}\ \tanh\left(\frac{\alpha E}{P_\mathrm{m}}\right) \tag{6}$$

Modeled values of P_m vary in both time and space:

$$P_\mathrm{m} = \Psi_S 3.5\times10^{-4}\ \exp[0.09T_0] \tag{7}$$

based on the local surface water temperature (T_0) and via an empirical function Ψ_s:

$$\Psi_s = 2.4 - 1.6\ \tanh\left[\frac{(S_0 - 12)}{4}\right] \tag{8}$$

where S_0 is the local, time-varying surface salinity. The exponential dependence of P_m on temperature is consistent with other observations from the Chesapeake Bay region (Gallegos, 2012) and the spatial variations driven by Ψ_s ensure higher productivity in the upper Bay with lower levels in the lower Bay driven by nutrient limitation (Harding et al., 1986; Malone et al., 1996). The ratio P_m/α sets the irradiance where photosynthesis becomes light saturated (E_k). Based on the analysis of the 7 years of near-surface oxygen data (Scully, 2018), we impose a simple linear relationship between the local surface temperature and E_k:

$$E_k = \frac{P_\mathrm{m}}{\alpha} = 4.9T_0 + 30 \tag{9}$$

This allows the saturating irradiance to vary in a manner consistent with the analysis of the surface oxygen data and results in a roughly linear relationship between P_m and α, consistent with other studies from Chesapeake Bay (e.g., Harding et al., 1986). The available light at any vertical location z is assumed to vary exponentially:

$$E = 0.43E_0 \exp[K_d z] \tag{10}$$

where K_d is the light attenuation coefficient and E_0 is the surface irradiance, which is set by the downwelling shortwave radiation from the atmospheric forcing. The factor 0.43 converts the downwelling shortwave radiation to photosynthetically active radiation (PAR; Fennel et al., 2006). Previous work in Chesapeake Bay

has demonstrated that light is attenuated by a number of constituents in the water column including total suspended solids (TSSs), chlorophyll, and chromophoric dissolved organic material (Kirk, 1994). Higher values of chromophoric dissolved organic material are found in low-salinity waters, and their influence on light attenuation is often parameterized in terms of salinity (Xu et al., 2005). Accurately modeling TSS is a complex and challenging endeavor involving a number of poorly constrained processes. We take a simplistic approach here, generally consistent with previous work in Chesapeake Bay, and model the light attenuation based on the surface salinity (S_0):

$$K_d = 0.8 + 2.2\ \exp[-0.18S_0] \tag{11}$$

In this formulation, light attenuation has a stronger dependence on salinity than previous relationships (Feng et al., 2015; Xu et al., 2005) because TSS is not modeled and we attempt to capture the fact that higher values of TSS are generally observed in the lower-salinity regions near the estuarine turbidity maximum.

Finally, a simple Gaussian formulation for temporal variations in CR is used:

$$\mathrm{CR} = \Psi_S 2.2\times10^{-4}\ \exp\left[\frac{-(\mathrm{days}-195)^2}{10,000}\right] \tag{12}$$

where "days" are the number of days since the beginning of the year. In time, this function peaks in mid-July (day = 195) and has the same spatial variability (Ψ_s) as P_m. The coefficient 2.2×10^{-4} was simply selected so that the spatially and annually averaged NEM is zero, consistent with an ecosystem where there is an exact balance between autotrophic and heterotrophic processes. Varying this value allows the model to easily shift between net heterotrophy and net autotrophy.

With this formulation, the model accounts for rates of GPP and CR that vary in both time and space (horizontally and vertically) consistent with observations from Chesapeake Bay. Tidal and wind-driven currents predicted by the circulation model interact with the spatial variations in the resulting oxygen field to provide a plausible representation of horizontal advection. Similarly, realistic contributions due to vertical mixing are simulated using the *k*-omega turbulence closure model with the stability functions of Kantha and Clayson (1994) and atmospheric gas exchange based on the wind speed-dependent formulation of Wanninkhof (2014). Obviously, the model is not a perfect representation of nature, but with these formulations it provides a reasonable representation of the contribution of both horizontal advection and vertical mixing on the DO dynamics.

4. Results

4.1. Model-Data Comparison

Before proceeding, it is worthwhile to demonstrate that this simplified model can reasonably simulate both temporal and spatial variations in DO in Chesapeake Bay. The model is compared to the surface data collected at the seven main stem Chesapeake Bay Interpretive Buoy System (CBIBS) locations (Figure 1) during 2013 and to the bottom oxygen data presented in Scully (2016b). The model has reasonable skill at simulating surface oxygen at all seven CBIBS locations (Figure 2 and Table 1). The model is biased low at the four central locations and biased high at the northern and southern limits, but overall these biases are small. An example of the model performance at the Annapolis buoy location over a 6-week period during summer demonstrates that the model captures the clear diurnal variability during this period, as well as some of the lower-frequency variations driven by variations in incoming solar radiation and physical mixing (Figure 3). The model captures the spatial variability in the magnitude of diurnal variability in a manner consistent with the observations (Table 1). The diurnal variability in the data decreases by roughly an order of magnitude from Patapsco to First Landing, and the model captures this strong decrease in diurnal variability moving down Bay.

The bottom oxygen data of Scully (2016b) do not resolve the full year but capture the onset of hypoxia in the spring and the subsequent ventilation in the fall. The model captures both the seasonal progression of bottom oxygen and some of the higher-frequency variability (Figure 4), and the model skill at all four bottom locations is high (Table 2). Previous work has demonstrated that a model with no biological variability can reasonably capture the seasonal cycle of hypoxia in Chesapeake Bay (Scully, 2013), demonstrating the first-

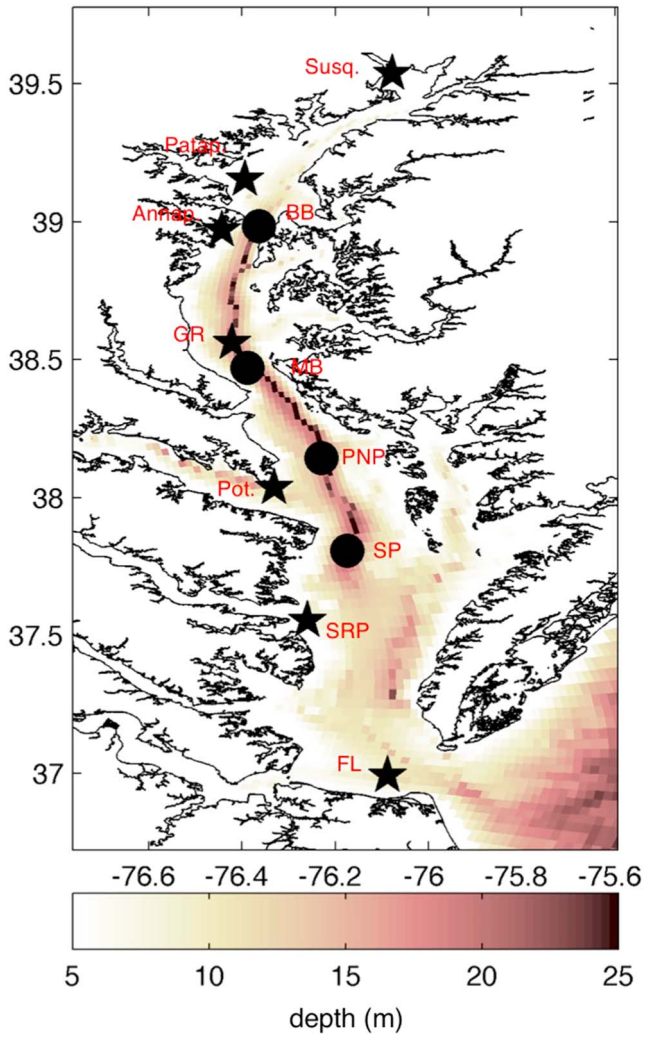

Figure 1. Model bathymetry with the locations of the CBIBS surface buoys (stars) and bottom oxygen measurements of Scully (2016b) (circles). CBIBS = Chesapeake Bay Interpretive Buoy System; Susq. = Susquehanna; Patap. = Patapsco; Annap. = Annapolis; BB = Bay Bridge; GR = Goose's Reef; MB = Mid Bay; PNP = Point No Point; Pot. = Potomac; SP = Smith Point; SRP = Stingray Point; FL = First Landing.

order control that physical processes play in controlling bottom oxygen dynamics. Here the inclusion of seasonal variations in oxygen production requires that the consumption of oxygen (CR) also vary seasonally in order to predict bottom oxygen with skill (equation (12)). It is important to note that capturing the strong vertical gradients in oxygen is necessary to accurately assess the importance of vertical mixing on variations of near-surface oxygen concentration.

4.2. Diel Method Evaluation

Having established the model's skill, the ability of the proposed method to quantify the underlying rate of GPP is evaluated next. The rate of GPP in the model is known, and we assume that the first-order influences of physical mixing and advection on the time variations of oxygen are reasonably captured. The primary goal is to assess if the proposed method can accurately quantify the local volumetric rate of GPP ($gO_2 \cdot m^{-3} \cdot s^{-1}$), as well as the underlying parameters of the *PE* curve (P_m and α), which can be used in conjunction with the depth of the surface mixed layer and vertical distribution of light to compute the more commonly reported depth-integrated values.

Estimates of GPP are compared for all seven of the CBIBS locations in the model for 2013 (Figure 5). The diel estimates are calculated from the modeled oxygen concentration at $z \sim -1 \pm 0.23$ m. Both the diel estimate and numerical model's GPP have been smoothed with 15-day boxcar filter to remove the diurnal variability caused by the daily cycle of irradiance. Plotted this way, the dominant variability is seasonal, which is well captured by the method. At all locations other than the Susquehanna buoy, the method predicts GPP with high skill and low bias (Table 3). Excluding the Susquehanna buoy, the Wilmott (1981) skill exceeds 0.92 at all buoys and the bias is less than 20%. At the Susquehanna buoy, the estimate of GPP is roughly a factor of 2 larger than the rate in the numerical model and the skill is much lower than the other locations (0.60).

The method was applied using the incoming solar radiation at the surface (E_0) and not the local in situ light predicted by the model via equation (10). In the model, the light varies vertically as dictated by the attenuation coefficient, which varies both spatially and in time via equation (11). Applying the method using the actual water column value of light (E), accounting for both the spatial and temporal variations in K_d, does not change the skill of the method in any appreciable way (Table 3). Using E_0 instead of E does reduce the inferred value of α, but these differences have no appreciable influence on the estimates of GPP due to the compensatory effect of the higher (nonattenuated) assumed value of PAR. This suggests that the method can be accurately applied to observing system data to estimate volumetric rates of GPP, when water column light attenuation is not measured, if a reasonable estimate of the surface irradiance can be obtained.

As will be discussed in detail below, there is an optimal vertical location where the method most accurately estimates the GPP. At this location, the method not only estimates GPP but also predicts the underlying variables of the *PE* curve with reasonable skill (Table 3). If we assume that the value of K_d is known (or measured), we can compute the vertically integrated production using measured surface irradiance combined with the estimates of P_m and α. Estimates of P_m are predicted with reasonable skill but are biased low at all seven locations (Table 3). Estimates of α have similar skill and are biased high, but the magnitude of the bias is reduced compared to P_m, except at the two northernmost locations. Even though the overall skill at predicting P_m and α is reduced compared to their combined effect on GPP (table), vertically integrated production is simulated with high skill (>0.94) at all seven CBIBS locations (Table 4). It is worth noting that the bias in the vertically

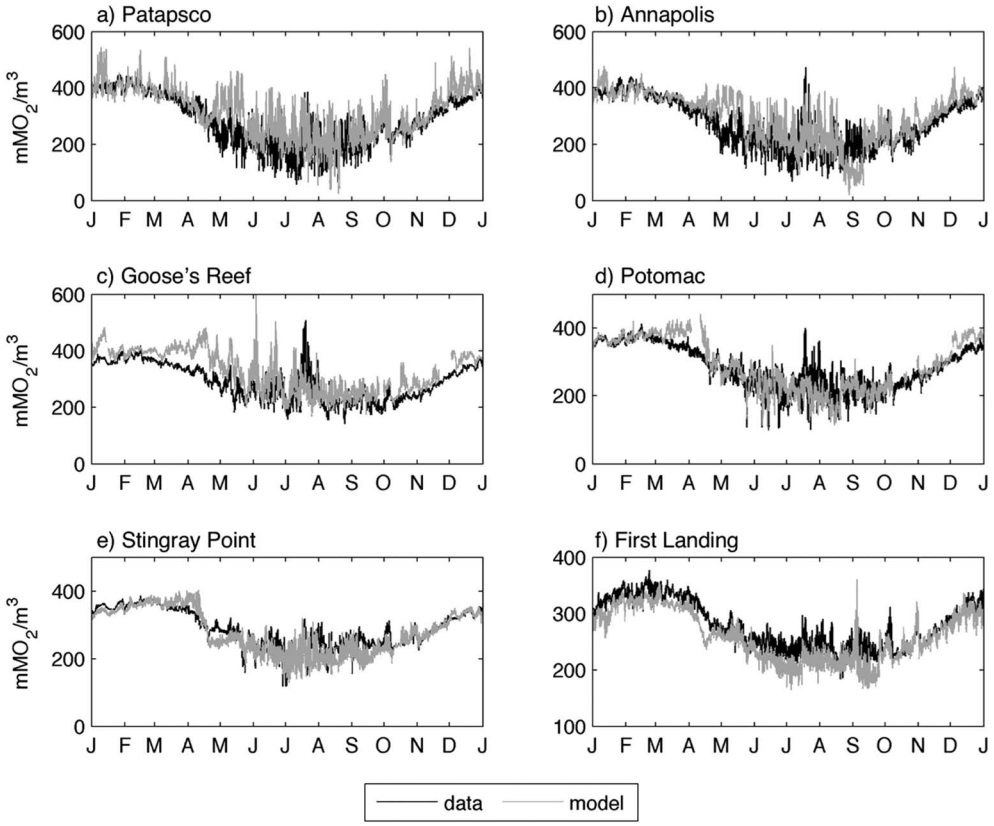

Figure 2. Comparison of surface oxygen concentration measured at the CBIBS buoys (black line) with the model simulation (gray line) for 2013. CBIBS = Chesapeake Bay Interpretive Buoy System.

integrated estimates of GPP at the Susquehanna location is reduced considerably compared to the bias in the volumetric rate at this location despite the relatively low skill at predicting the *PE* curve. At this location, integrated GPP is predicted with high skill even though the vertical structure is poorly predicted, consistent with compensatory errors in P_m and α. These estimates of integrated GPP ignore the role that changes in the surface mixed layer have on the light that the phytoplankton experience, which is equivalent to assuming that the photic depth is always shallower than the surface mixed-layer depth. This is clearly a simplification, but it is consistent with how GPP is accounted for in most biogeochemical models.

This analysis has focused on the locations in the model that coincide with the CBIBS buoy locations. We next extend the analysis to the entire model domain. Figure 6 compares the rate of GPP in the numerical model to

Table 1
Skill Assessment of Modeled Surface Oxygen Concentration for 2013 at the Seven CBIBS Buoy Locations Including Wilmott (1981) Skill, Normalized Mean Bias, and Comparison of the Observed and Modeled Diurnal Variance in Surface Oxygen Calculated From Band-Pass-Filtered Data

Location	Wilmott score	Normalized mean bias	Diurnal variance (data) [$mMO_2/m^3]^2$	Diurnal variance (model) [$mMO_2/m^3]^2$
Susquehanna	0.91	0.03	69.1	96.1
Patapsco	0.89	−0.09	455.1	416.3
Annapolis	0.90	−0.08	280.0	377.4
Goose's Reef	0.84	−0.13	209.2	145.1
Potomac	0.93	−0.02	62.5	103.0
Stingray Point	0.94	0.03	80.1	53.1
First Landing	0.92	0.07	35.4	36.2

Note. Pass band of 1/20 and 1/28 hr^{-1}. Wilmott skill for a model variable X with mean $<X>$ is defined as follows: Skill $= 1 - \frac{\Sigma|X_{mod}-X_{obs}|^2}{\Sigma[|X_{mod}-X_{obs}|+|X_{obs}-X_{obs}|]^2}$. CBIBS = Chesapeake Bay Interpretive Buoy System.

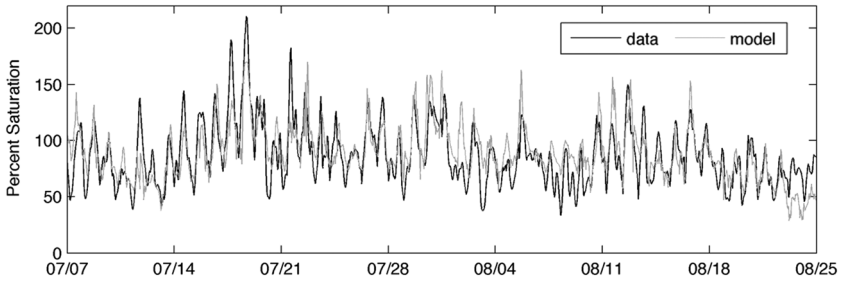

Figure 3. Detailed model-data comparison of surface oxygen percent saturation at the Annapolis buoy location for summer 2013. There is good agreement between the observations (black line) and the model (gray line) at both diurnal and lower frequency.

the inferred rate obtained by applying the diel method to the modeled time rate of change of oxygen at every location in the model domain at a depth of $z \sim -1$ m. This analysis allows us to evaluate the method's ability to estimate spatial variations in GPP, as well as how well the method captures temporal variations at different locations throughout the Bay. As with the analysis at the CBIBS locations, the Bay-wide skill does not change appreciably if the surface irradiance is used instead of the locally attenuated value. A comparison of the annually averaged GPP demonstrates that the method extracts spatial patterns that are generally consistent with the spatial distribution in the numerical model (Table 5). Overall, the estimated rates of GPP are biased low by 6%, but there are regions where the volumetric rate GPP is significantly overestimated, specifically the shallow upper-Bay region north of 39.3°N (Figure 7a). Consistent with the analysis at the Susquehanna buoy location, even when the volumetric rate is overestimated, the vertically integrated value

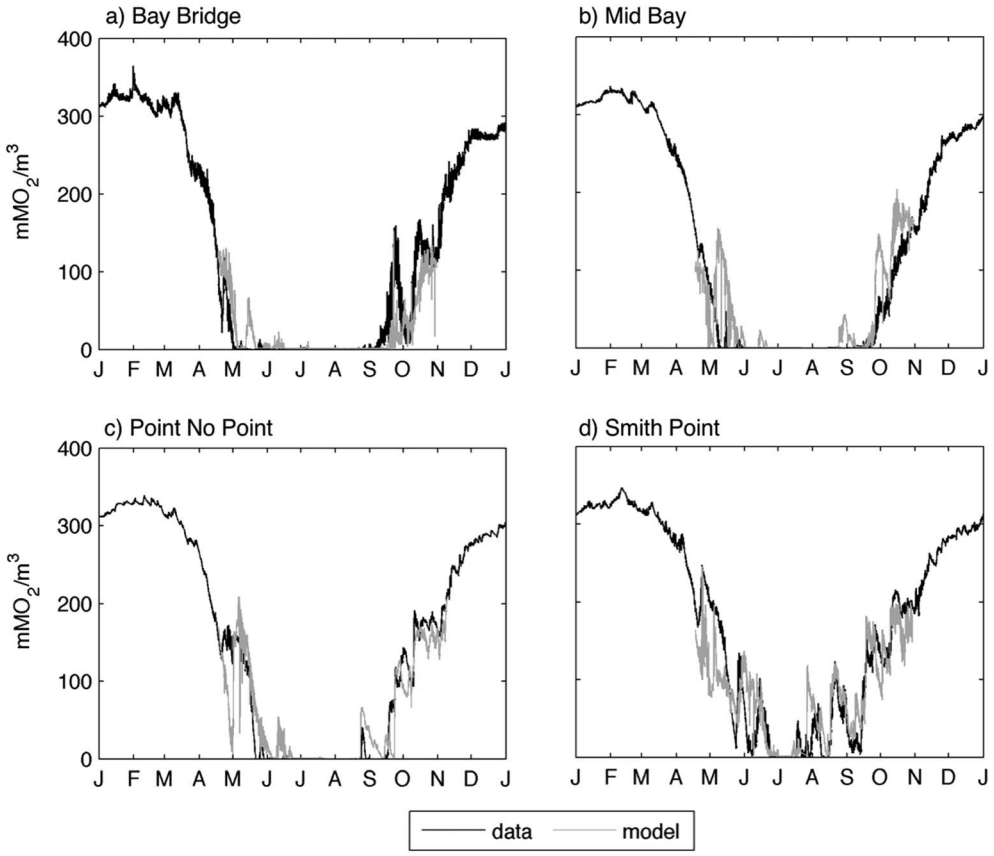

Figure 4. Comparison of bottom oxygen concentration measured by Scully (2016b) at four deep channel locations (black line) with the model simulation (gray line) for 2013. Model captures seasonal cycle of hypoxia as well as some of the higher-frequency variability with high skill.

Table 2
Skill Assessment of Modeled Bottom Oxygen Concentration for 2013 Compared to the Data of Scully (2016b)

Location	Wilmott score	Normalized mean bias
Bay Bridge	0.87	0.14
Mid Bay	0.85	−0.38
Point No Point	0.94	0.00
Smith Point	0.90	0.03

compares favorably (Figure 7b). The large errors in the volumetric rate in the low-salinity upper-Bay regions occur where the surface mixed layer is deeper than the euphotic zone (Figure 7c). Errors in both the volumetric and vertically integrated rates are small over most of middle and lower Bay, and the overall along-Bay variation in GPP is well represented. The skill of the method at capturing temporal (mainly seasonal) variations at any location within the domain is generally high, indicating that the method can reasonably predict the underlying seasonal variability at most locations (Table 5).

Using the water column value of irradiance allows for a quantitative comparison between the estimated and "real" values of the *PE* curve. With the exception of the low-salinity region north of 39.3°N, the method extracts both α and P_m with reasonable skill, including both spatial and temporal variability (Figure 8 and Table 3). In the low-salinity upper Bay where the surface mixed layer is deeper than the euphotic depth, errors in α are large (data not shown), but in the rest of the Bay, α is predicted with reasonable accuracy. P_m is underpredicted, but given the light-limited nature of GPP that is simulated, the ability to predict GPP is controlled by α to a much greater extent than by P_m.

5. Discussion

Given the spatial complexity in the oxygen field driven by both biological and physical processes, it is worth demonstrating why the inferred GPP from the diel method has high skill and low bias, even though advection and mixing significantly impact the observed time rate of change of oxygen. To illustrate this more clearly,

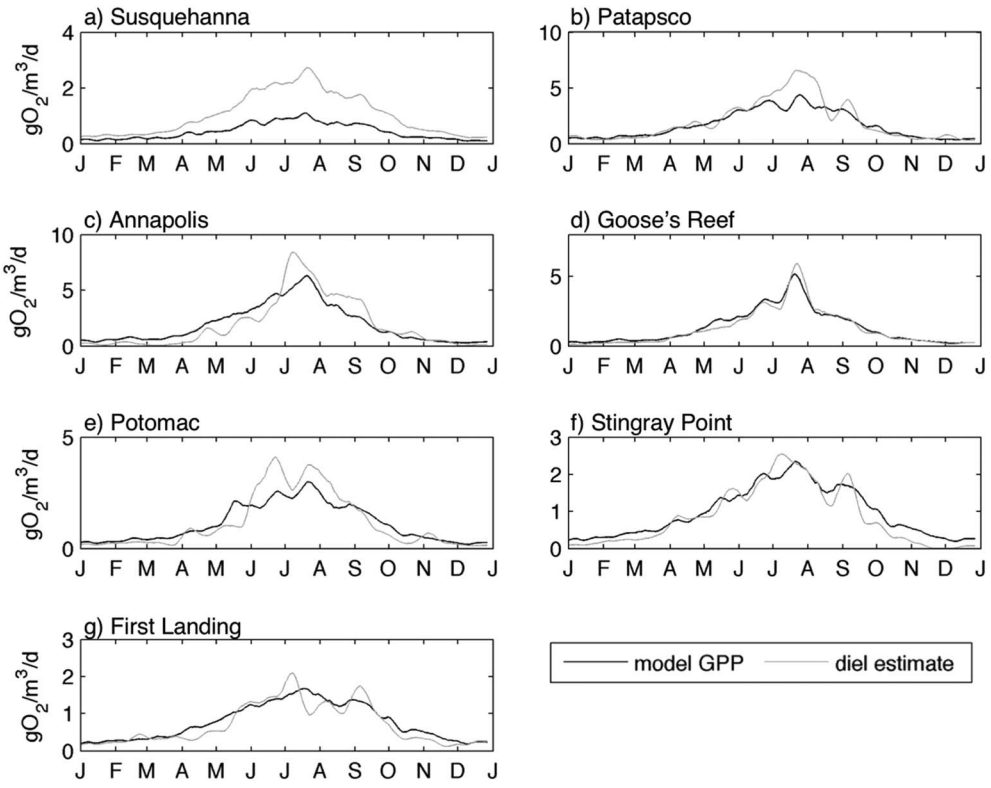

Figure 5. Comparison of volumetric rate of GPP from the numerical model (black line) with the diel estimate based on the time rate of change of oxygen at $z \sim -1.0$ m (gray line) for all seven CBIBS buoy locations. Both GPP and the diel estimate have been smoothed with a running 15-day filter to remove diurnal variability and to match the temporal resolution of the diel estimate of the *PE* curve parameters. The method has high skill and low bias at all locations other than the Susquehanna buoy. GPP = gross primary production; CBIBS = Chesapeake Bay Interpretive Buoy System; *PE* = photosynthesis-irradiance response.

Table 3
Skill Assessment of the Proposed Diel Method for the Volumetric Rate of GPP and the Parameters of the PE Curve (P_m and α) at the Seven CBIBS Buoy Locations

	Surface irradiance (E_0)						Attenuated irradiance (E)					
	GPP		P_m		α		GPP		P_m		α	
Location	Skill	Bias	Skill	Bias	Skill	Bias	Skill	Bias	Skill	Bias	Skill	Bias
Susquehanna	0.60	1.38	0.56	−0.80	NA	NA	0.63	1.23	0.53	−0.82	0.32	1.94
Patapsco	0.92	0.17	0.79	−0.43	NA	NA	0.93	0.17	0.83	−0.40	0.74	0.43
Annapolis	0.94	0.00	0.93	−0.27	NA	NA	0.94	0.01	0.85	−0.36	0.78	0.18
Goose's Reef	0.99	−0.06	0.98	−0.19	NA	NA	0.99	−0.07	0.96	−0.25	0.97	0.00
Potomac	0.93	0.04	0.89	−0.08	NA	NA	0.93	0.05	0.88	−0.09	0.80	0.10
Stingray Point	0.97	−0.12	0.94	−0.10	NA	NA	0.97	−0.12	0.94	−0.06	0.80	−0.17
First Landing	0.96	−0.08	0.78	−0.23	NA	NA	0.96	−0.08	0.76	−0.19	0.78	0.03

Note. The diel estimates were obtained by applying the method to the time rate of change of oxygen at $z \sim -1$ m and are compared to the known parameters from the model. Reported are the Wilmott (1981) skill and the normalized mean bias based on application of the method using the surface irradiance (left-hand columns) and using the local (attenuated) water column irradiance at $z \sim -1$ m. GPP = gross primary production; *PE* = photosynthesis-irradiance response; CBIBS = Chesapeake Bay Interpretive Buoy System; NA = not applicable.

near-surface model output from the Goose's Reef buoy location is analyzed. The oxygen balance (equation (1)) is evaluated at a variety of time scales to help show why the proposed method can reasonably estimate the underlying rate of GPP. To begin with, a 15-day period in July is analyzed and the terms in the oxygen balance at $z \sim -1$ m are averaged as a function of the M2 tidal phase (Figure 9a). Averaged in this way, $\partial O_2/\partial t$ is strongly correlated with the advective term. Oxygen concentrations generally decrease during the flood tide and increase during the ebb, consistent with lower surface oxygen concentration down Bay from this location in the model. Over this 15-day period, neither the primary production nor the divergence in vertical flux (mixing term) exhibits significant semidiurnal variability, and these two terms are roughly equal and opposite.

The data are averaged next as a function of the hour of the day in order to highlight the diurnal variability (Figure 9b). Averaged in this way, the time rate of change of oxygen and primary production have a strong positive correlation. Advection and mixing are both negative, on average, and exhibit little diurnal variability. The weak diurnal variations in mixing are largely out of phase with $\partial O_2/\partial t$ during this period. The diel method exploits this positive correlation between GPP and the incoming solar radiation, and the method accurately estimates GPP not because advection and mixing are weak but because they are not correlated with solar radiation. The primary tidal constituent in Chesapeake Bay is the semidiurnal M2, which moves in and out of phase with the diurnal solar forcing over the fortnightly cycle. Therefore, to avoid any potential aliasing due to tidal advection, the method is best applied to intervals of ~15 days. This ensures that there is minimal correlation between semidiurnal tidal processes and the diurnal solar forcing.

Table 4
Skill Assessment of the Proposed Diel Method for the Vertically Integrated Rate of GPP Derived Using the Observed Vertical Distribution of Light and the PE Curve Parameters Estimated Using the Diel Method at $z \sim -1$ m at the Seven CBIBS Buoy Locations

Location	Skill	Bias
Susquehanna	0.97	−0.16
Patapsco	0.97	0.04
Annapolis	0.95	−0.03
Goose's Reef	0.99	−0.08
Potomac	0.94	0.04
Stingray Point	0.97	0.11
First Landing	0.96	−0.08

Note. GPP = gross primary production; *PE* = photosynthesis-irradiance response; CBIBS = Chesapeake Bay Interpretive Buoy System.

It is important to point out that the empirical formulations for GPP and CR both rely on expressions that are functions of the surface salinity. This ensures spatial variability in GPP that is generally consistent with observations. The formulation for GPP depends much more strongly on light than on salinity, and tidal variations in salinity contribute essentially no high-frequency variability to the time series of GPP. The semidiurnal variations in $\partial O_2/\partial t$ are driven by horizontal advection but not influenced in any significant way by tidal variations in surface salinity.

At time scales longer than a few days, the time rate of change of oxygen is not a dominant term in the oxygen evolution equation. At these time scales, the dominant balance near the ocean surface is between primary production and the vertical divergence in turbulent oxygen flux (Figure 9c). In the simplest terms, primary production is acting to create a profile of oxygen that exponentially decays in the vertical, and vertical mixing is acting to homogenize this profile. As a result, throughout most of the surface mixed layer, the vertical flux of oxygen is downward

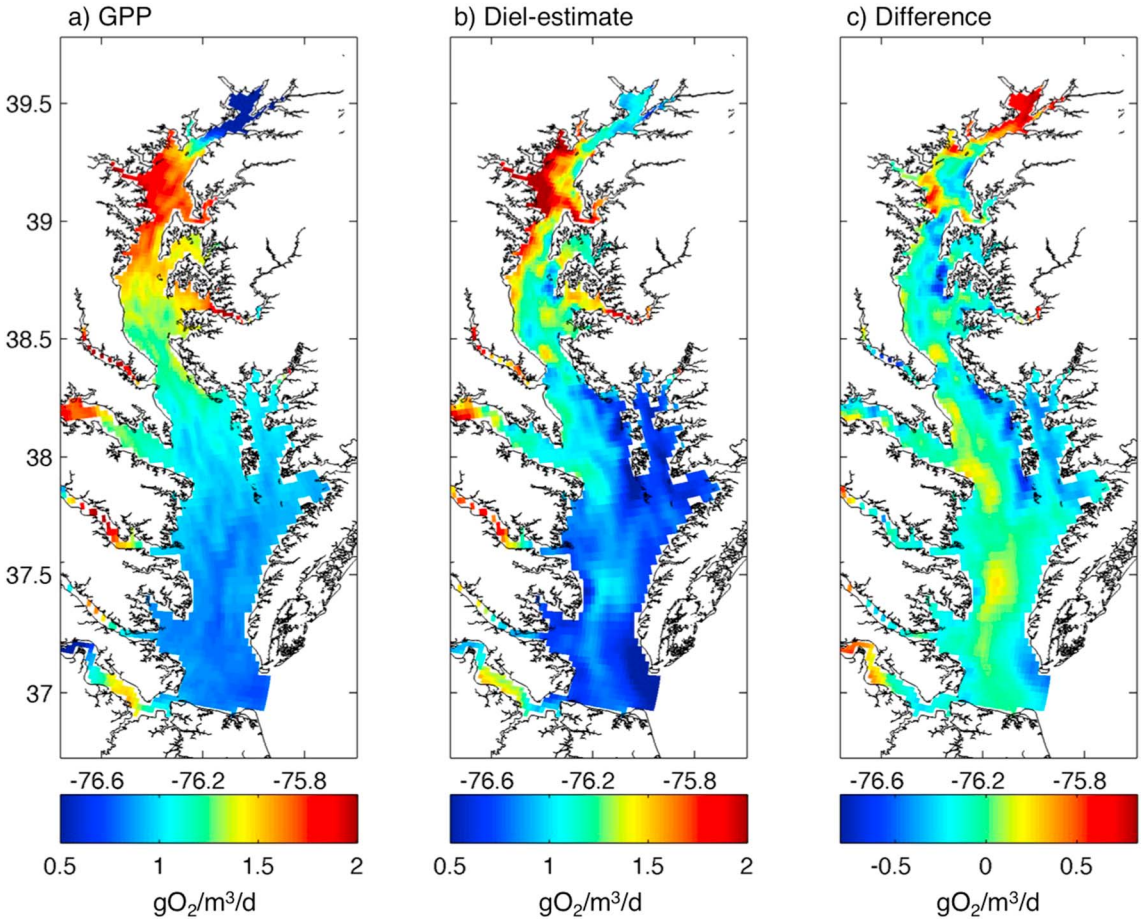

Figure 6. Comparison of (a) the annually averaged volumetric rate of GPP imposed in the numerical model at $z \sim -1$ m with (b) the diel estimate based on the time rate of change of oxygen at $z \sim -1.0$ m and (c) the difference (method minus model). CR has similar spatial distribution and the NEM in the model is set to zero. GPP = gross primary production; CR = community respiration; NEM = net ecosystem metabolism.

(Figure 10a). The exception is the region immediately adjacent to the sea surface, where supersaturated conditions lead to an outward air-sea gas flux. The surface flux and the flux at $z \sim -1$ m often have the opposite sign, and this strong divergence in vertical flux is the dominant term that balances primary production in this near-surface region (Figure 10b).

A primary reason the proposed method works is the lack of correlation between mixing and advection and the diurnal solar forcing. Another way of stating this is that the sum of advection, mixing, and CR during the nighttime hours ($\Delta\widehat{O_2}$) must be representative of their contribution during daylight hours (ΔO_2). If any of these terms contribute significantly to diurnal changes in $\partial O_2/\partial t$, the estimates from the diel method will be biased.

Table 5
Skill Assessment of the Proposed Diel Method Applied at z ~ −1 m for All Locations Within the Model Domain

GPP			P_m			α			Integrated GPP		
Skill		Mean bias	Skill		Median bias	Skill		Median bias	Skill		Median bias
Space	Time		Space	Time		Space	Time		Space	Time	
0.81	0.92	−0.06	0.64	0.84	−0.25	0.55	0.77	0.03	0.85	0.89	−0.09

Note. The Wilmott skill is reported for spatial variations (calculated from the annually averaged values at all model locations) and temporal variations (mean of skill based on temporal variations at each location). The median normalized bias also is reported (averaged in both time and space for the entire domain). Assessment is reported for volumetric rate of GPP, *PE* curve parameters, and the vertically-integrated GPP. GPP = gross primary production; *PE* = photosynthesis-irradiance response.

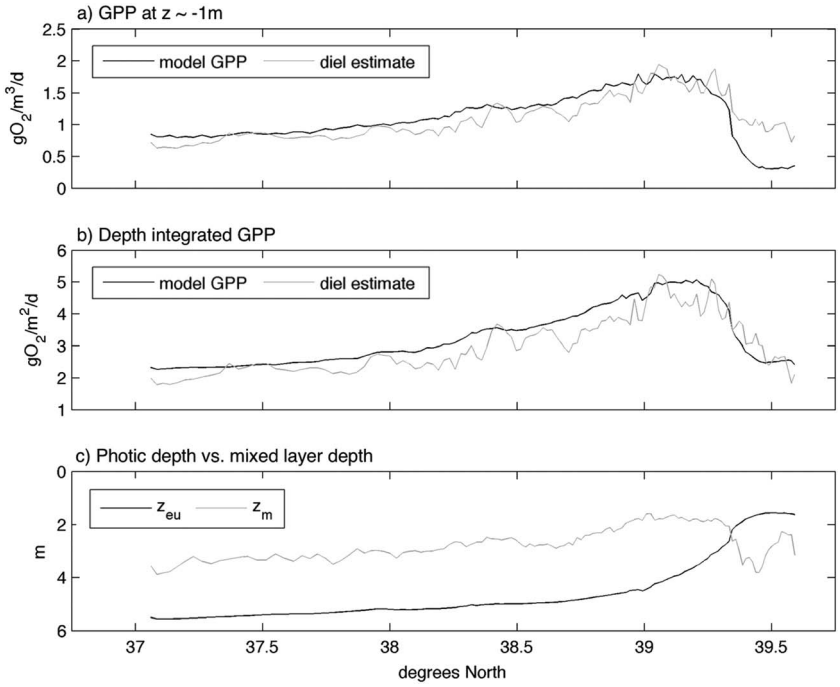

Figure 7. (a) Comparison of the annually averaged volumetric rate of GPP from the numerical model averaged as a function of the along-Bay location (black line) with a similar average from the diel estimate based on the time rate of change of oxygen at $z \sim -1.0$ m (gray line). (b) Comparison of the annually averaged vertically integrated rate of GPP from the numerical model averaged as a function of the along-Bay location (black line) with a similar average from the diel estimate using the *PE* curve estimated at a depth of $z \sim -1.0$ m (gray line). (c) Comparison of the annually averaged depth of the photic zone (black line) and surface mixed-layer depth (gray line) averaged as a function of the along-Bay location. The mixed-layer depth is calculated from the depth where the turbulent diffusivity becomes equivalent to the background diffusivity specified in the model. GPP = gross primary production; *PE* = photosynthesis-irradiance response.

While the diurnal variability in the mixing term is relatively small at $z \sim -1$ m, this is not true throughout the surface mixed layer. Closer to the surface, there is a divergence in turbulent oxygen flux at diurnal time scales driven by the outward surface flux and the strong downward flux near the surface (Figure 11a). This diurnal contribution due to divergent turbulent flux acts to reduce the diurnal variability in $\partial O_2/\partial t$ close to the surface. Deeper in the surface mixed layer, there is a convergence in turbulent oxygen flux driven by the downward flux from the overlying water column and the zero-flux condition at the base of the surface mixed layer,

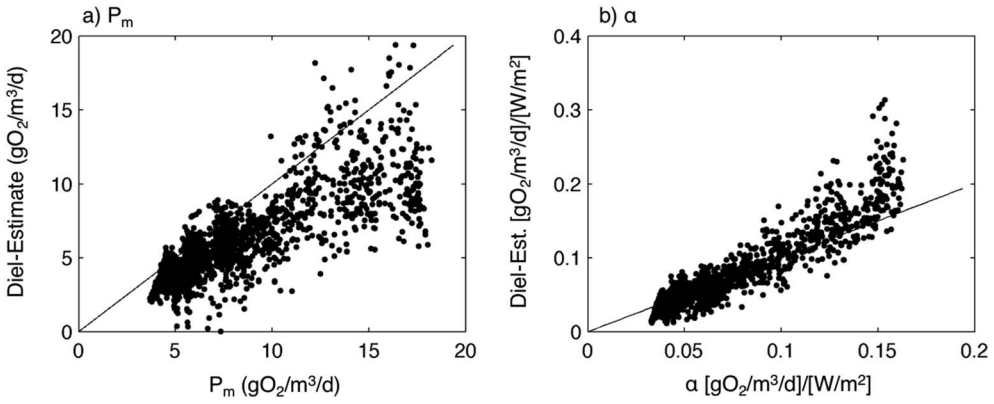

Figure 8. Comparison of the value of (a) P_m and (b) α used in the numerical model with the estimated values from the diel method from a depth of $z \sim -1$ m for all locations within the Bay where salinity is greater than 5. All values are annual averages. Black line is 1:1 in both panels. There is high bias in the estimates of α for all locations where salinity is lower than 5 as discussed in the text, and these data are not shown here.

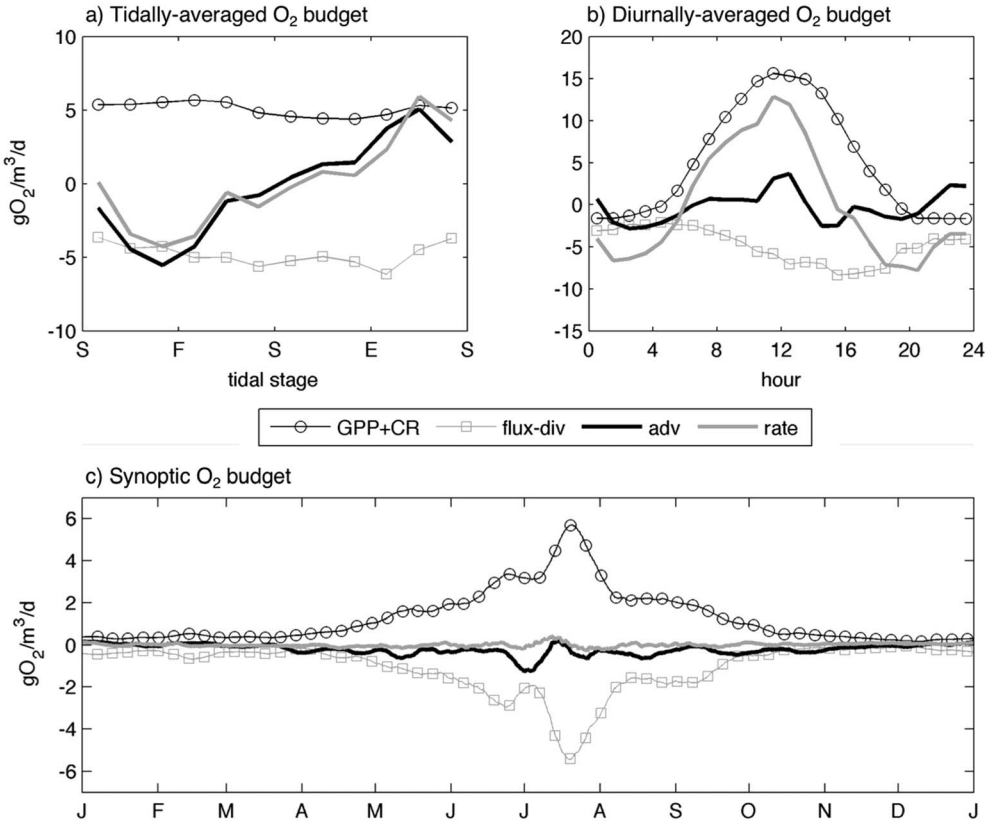

Figure 9. Evaluation of the oxygen budget at $z \sim -1$ m from the model location that corresponds with the Goose's Reef buoy (a) averaged as a function of the M2 tidal phase during 10–25 July 2013; (b) averaged as a function of the hour of the day during 10–25 July 2013; and (c) for the entire year after smoothing with a 15-day boxcar filter. In all plots the sum of GPP and CR are plotted as circles, the vertical flux divergence as squares, the advective terms with a thick black line, and the time rate of change of oxygen with a thick gray line. In Figure 9a the tidal stage is indicated as flood (F), ebb (E), or slack (S) based on the M2 tidal velocity. GPP = gross primary production; CR = community respiration.

which acts to enhance the diurnal variations in $\partial O_2/\partial t$ (Figure 11c). This diurnal variability induced by turbulent mixing will result in significant errors for open-water techniques such as the Fourier method proposed by Cox et al. (2015), which employs a frequency-based approach that assumes that all of the diurnal variability is due to GPP.

The vertical structure and diurnal variations of the flux divergence results in an underprediction of GPP when the method is applied very close to the surface and an overprediction near the base of the euphotic zone (Figure 12a). The ideal vertical location will coincide with the location where the local value of GPP equals the average value over the surface mixed layer. For light-limited conditions ($E < E_k$) where the model predicts an exponential profile of GPP, this location will be set by the vertical light attenuation and will occur where $z \sim -1.54/K_d$. If the surface mixed-layer depth is shallower than the euphotic depth, this location is closer to the surface, and when the surface mixed-layer depth is deeper than the euphotic zone, this location is deeper.

More generally, errors in the method associated with vertical mixing will be minimized when the surface mixed-layer depth is much shallower than the euphotic depth. Under these conditions, vertical mixing is acting on a smaller range of the vertical gradient in GPP, which effectively reduces the magnitude of the error associated with mixing within the surface mixed layer. Conversely, when the surface mixed-layer depth is equal to or deeper than the euphotic zone, vertical mixing will act over the entire vertical gradient in GPP and the magnitude of the errors associated with mixing will be enhanced. Under these conditions, the magnitude of the error is enhanced, but the sign of the error is determined by the vertical location, with underprediction closer to the surface and overprediction near the base of the surface mixed layer.

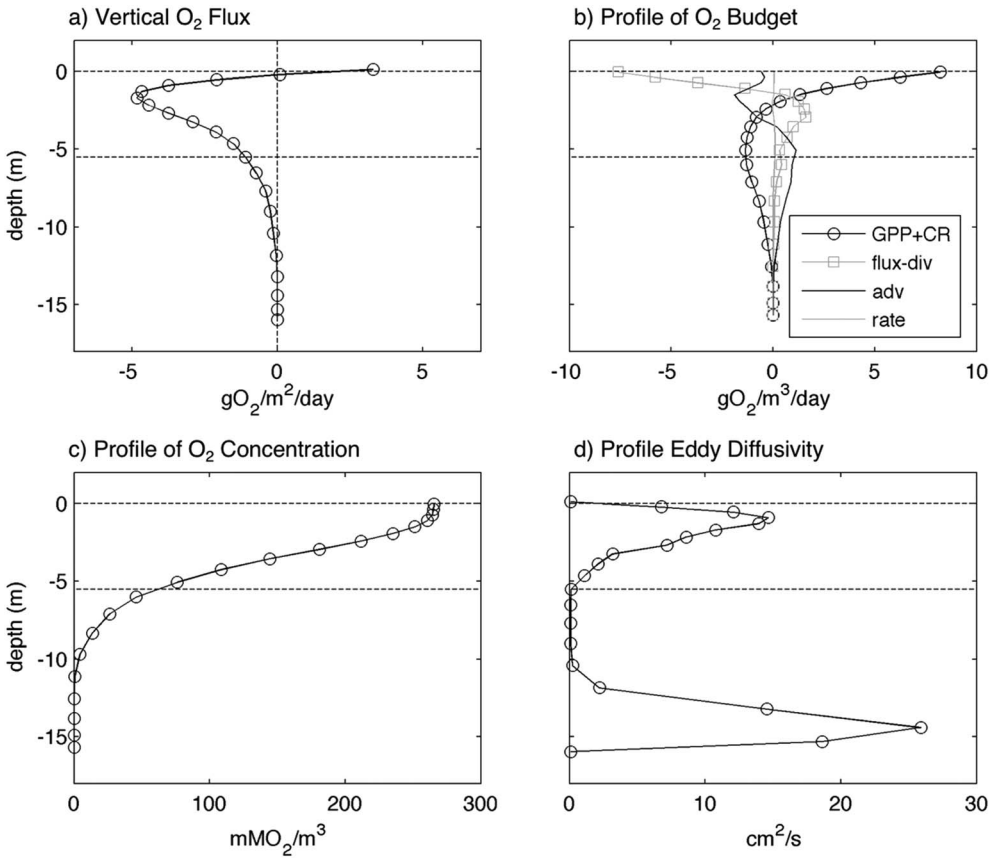

Figure 10. Vertical profiles from the model location that corresponds with the Goose's Reef buoy location including the following: (a) the vertical oxygen flux; (b) the terms in the oxygen budget; (c) oxygen concentration; and (d) eddy diffusivity. All values have been averaged over the month of July, and in all panels the horizontal dashed lines represent the sea surface and the base of the surface mixed layer inferred from the eddy diffusivity. In Figure 10b the sum of GPP and CR are plotted as circles, the vertical flux divergence as squares, the advective terms as a black line, and the time rate of change of oxygen as a gray line. Note the strong flux divergence near the surface caused by the outward surface flux and strong downward flux at $z \sim -1$ m. GPP = gross primary production; CR = community respiration.

The region of greatest bias in the diel estimates of GPP is in the low-salinity regions of the upper Bay near the location of the Susquehanna buoy (Figures 6 and 7). This is a region where the surface mixed layer is deeper than the euphotic zone on average (Figure 7c). This generally increases the magnitude of the error in this region. The combination of shallower water, reduced stratification, and higher suspended sediment increases both K_d and z_{mix} in the estuarine turbidity maximum region. The evaluation of the method was performed at $z \sim -1$ m, which is deeper than the ideal vertical location for the upper Bay region where $K_d > 1.54$. This results in an overprediction of GPP because diurnal variations in the flux divergence term are positively correlated with the diurnal variations in light at this depth. While the fact that the estimates are high in this region is caused by the vertical position, the increased magnitude of error is related to the fact that the surface mixed layer is deeper than the euphotic zone.

The errors associated with vertical mixing are enhanced when there is a strong vertical gradient in GPP, such as the assumed exponential profile under light-limited conditions that is employed in the model. The overall error would be diminished considerably if GPP had less vertical variability. For instance, if GPP was constant in the vertical over the entire euphotic depth, the errors associated with vertical position would be greatly diminished. Similarly, light-saturated conditions ($E > E_k$) will result in near-surface values of GPP that are more uniform in the vertical. This reduces the tendency of GPP to create vertical gradients in oxygen, and the corresponding divergence in the vertical flux also would be significantly reduced. Thus, the bias due to mixing is less under light-saturated conditions and errors associated with vertical position within the surface mixed layer are diminished.

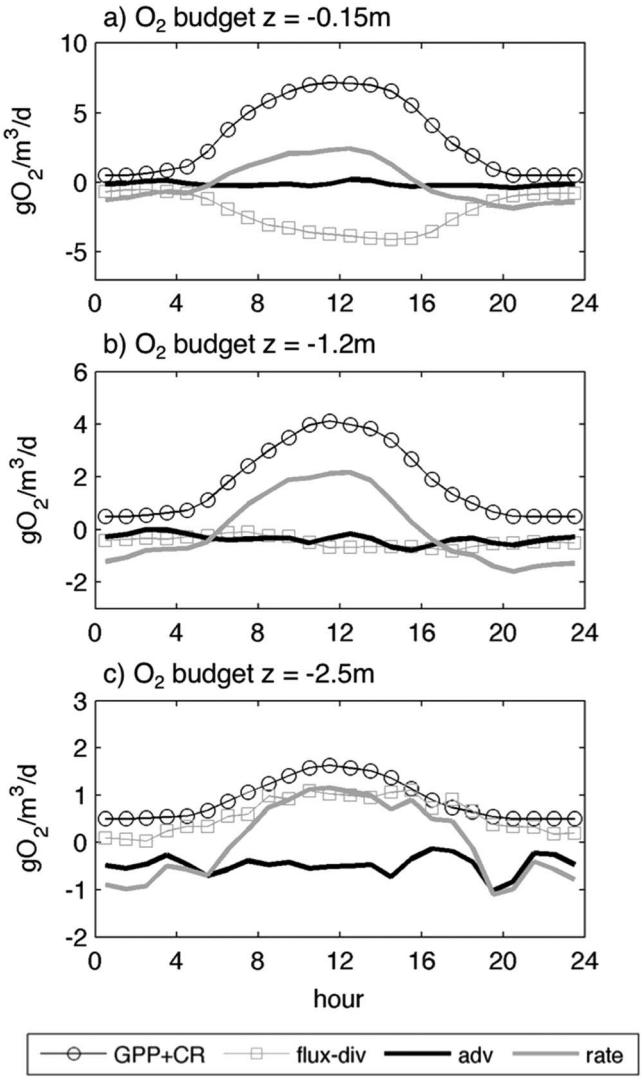

Figure 11. Terms in the oxygen budget from (a) $z \sim -0.15$ m, (b) $z \sim -1.2$ m, and (c) $z \sim -2.5$ m from the model location that corresponds with the Goose's Reef buoy location. The data are averaged as a function of the hour of the day over the entire year. The sum of GPP and CR are plotted as circles, the vertical flux divergence as squares, the advective terms as a black line, and the time rate of change of oxygen as a gray line. The flux divergence term is out of phase with the GPP + CR and the time rate of change at $z \sim -0.15$ m and in phase at $z \sim -2.5$ m. GPP = gross primary production; CR = community respiration.

There are a number of reasons why natural profiles of GPP are likely to be more uniform in the vertical than the formulation used in the model. The model used here does not realistically account for how turbulent mixing effects the light phytoplankton experience. The simple formulation of the *PE* curve in the model does not account for photoinhibition, photoadaptation, or vertical variations in α and P_m, all of which have been demonstrated in field observations (Behrenfeld et al., 2004; MacIntyre et al., 2002). Turbulent mixing fundamentally controls the light experienced by individual phytoplankton and photoadaptation occurs at a variety of time scales. Under weak turbulent mixing, even relatively slow adapting parameters such as P_m are expected to develop vertical gradients within the surface mixed layer (e.g., Lewis et al., 1984). Values of E_k often are observed to decrease with depth (Behrenfeld et al., 2004), and this vertical variation in the PE curve would act to reduce the vertical gradient in GPP. Falkowski and Wirick (1981) used a random walk model to account for the interactions between turbulent mixing and photoadaptation to suggest that while vertical mixing does significantly alter the depth-integrated rate of GPP, it can effectively reduce the vertical gradient in GPP when photoadaptation occurs. Similarly, photoinhibition near the surface also would act to reduce the vertical gradient in GPP.

Regardless of the mechanism, a more realistic representation of the interactions between vertical mixing and phytoplankton photophysiology is likely to reduce the vertical gradients in GPP compared to the assumed exponential profile used in the model. Therefore, the static representation of GPP used in the model most likely represents an upper limit on the errors caused by vertical mixing on diel variations in oxygen. One consequence of the strong vertical gradient in GPP is an overall reduction in the diurnal variability in the time rate of change of oxygen near the surface (e.g., Figure 11a). As noted in Scully (2018), the correlations between the NARR model of incoming solar radiation and the field observations of $\partial O_2/\partial t$ at the CBIBS buoys are higher than for the same analysis performed on the model output at these locations. This higher correlation occurs in spite of the fact that the NARR radiation is used to force GPP in the model and is only an estimate for the surface radiation incident at the buoy locations. This greater correlation with the CBIBS observations as compared to the model could be caused by a number of deficiencies in the underlying model but is consistent with reduced correlation in the model driven by vertical mixing near the surface.

The influence of mixing on diel variations of oxygen has long been recognized, and methods have been proposed to "correct" the observed time rate of change of oxygen by assuming that the contribution of the flux divergence can be estimated as F_{surf}/z_{mix} (Cole et al., 2000; Coloso et al., 2008; Cox et al., 2015; Van de Bogert et al., 2007). This correction is based on the fact that that there is no vertical flux through the base of the surface mixed layer ($z = -z_{mix}$), and the average flux divergence over this region is equal to F_{surf}/z_{mix}. In order for this approach to be valid for measurements of oxygen at a fixed vertical location, the oxygen concentration must have no vertical variation throughout the surface mixed layer. Only when this is true will the time rate of change of oxygen at a fixed vertical position accurately represent the average rate over the surface mixed layer. In addition, both F_{surf} and z_{mix} must be accurately known—two quantities that are notoriously difficult to directly measure. If these conditions are satisfied and there is no horizontal or vertical advection, then the surface "correction" can be applied so that the mean rate of GPP averaged over the surface mixed layer can be calculated. However, only in a vertically integrated sense does F_{surf}/z_{mix} accurately represent the average flux divergence in the surface mixed layer. As seen in Figure 10b, the flux

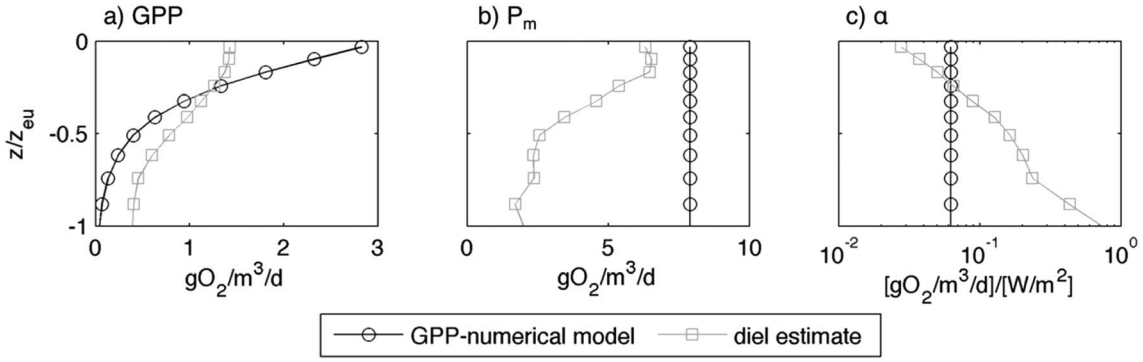

Figure 12. Vertical profiles of (a) GPP, (b) P_m, and (c) α from the model location that corresponds to the Goose's Reef buoy plot as a function of optical depth. The "real" values imposed in the model are plotted as the black circles, and the estimates from the diel method are plotted as the gray squares. Near the surface, P_m is consistently underpredicted, and the bias in α shows a strong vertical dependence with minimal bias at $z/z_{eu} \sim 0.2$. GPP = gross primary production.

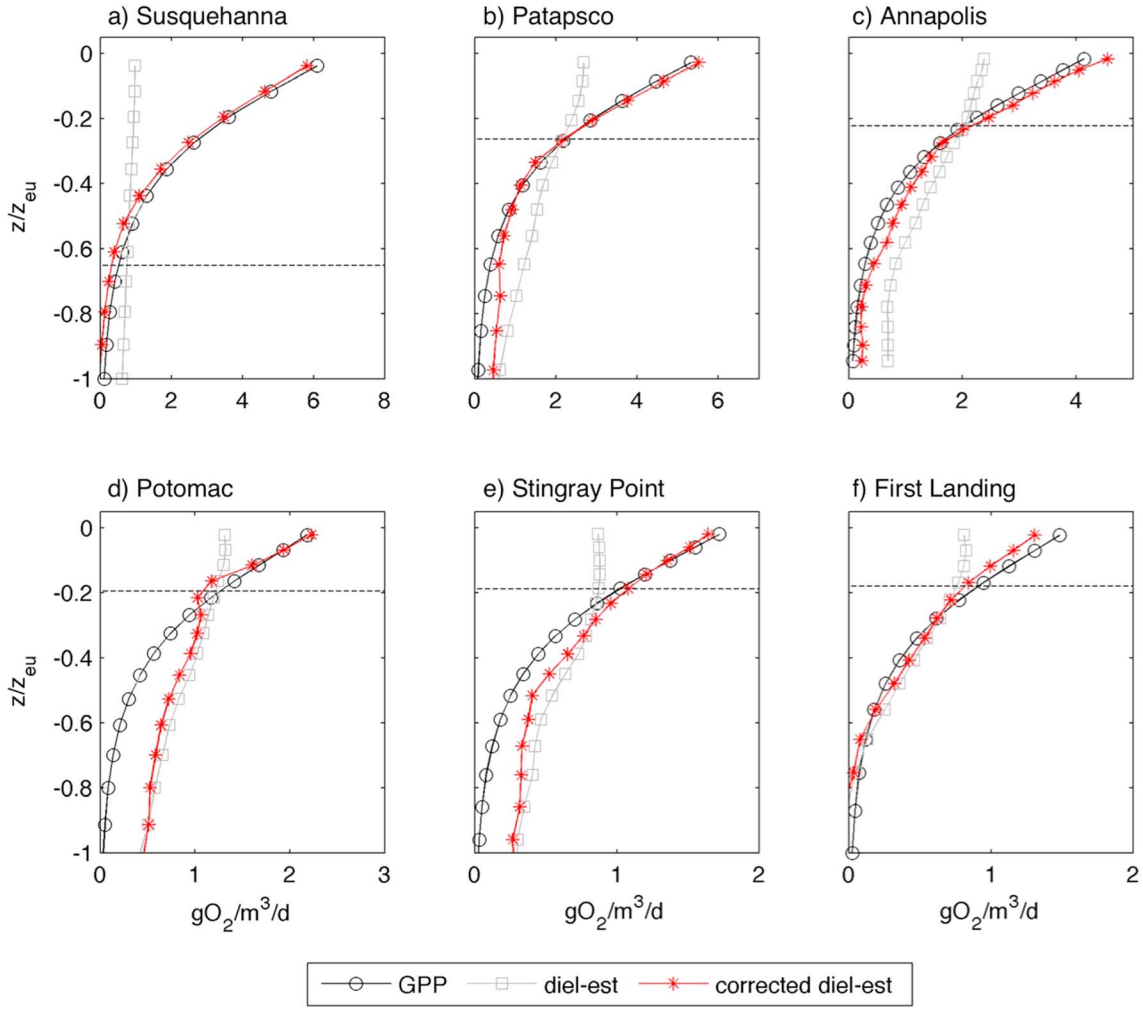

Figure 13. Vertical profiles of GPP from the numerical model (black circles), diel estimates based on the time rate of change of oxygen from the model (gray squares), and diel estimates based on the time rate of change of oxygen from the model that have been "corrected" using the local vertical turbulent flux divergence (red asterisks) for six CBIBS locations. The profiles are plotted as a function of optical depth, and the horizontal dashed line represents the location where $z \sim -1$ m. Correcting the time rate of change using the turbulent flux divergence reduces nearly all of the bias observed immediately below the sea surface. GPP = gross primary production; CBIBS = Chesapeake Bay Interpretive Buoy System.

divergence changes sign from the top to bottom of the surface mixed layer, and F_{surf}/z_{mix} is a very poor representation of the local flux divergence at any point within this region. Furthermore, it is overly simplistic to assume that the depth of the surface mixed layer can be accurately estimated from regions of vertically uniform oxygen, temperature, or salinity distribution, as is typically done (e.g., Cole et al., 2000). Advective process, and biological production in the case of oxygen, can result in appreciable vertical gradients within the surface mixed layer (Figure 10c). This not only invalidates the assumption of uniform concentration throughout the surface mixed layer but also will result in significant errors in the estimate of z_{mix}. As a result, application of the surface flux "correction" is not appropriate for the estuarine conditions simulated in this model and may not be valid more generally when GPP varies significantly in the vertical.

A much more robust alternative to the surface flux correction is direct measurements of the local flux divergence. Recent advances using fast-response oxygen optodes have demonstrated the ability to successfully measure turbulent oxygen fluxes near the ocean surface (e.g., Long & Nicholson, 2017). Given the large fluxes and strong vertical gradients in flux that are expected (Figure 10a), such techniques could potentially measure the flux divergence with suitable accuracy to more effectively correct the observed time rate of change of oxygen for the influence of mixing. To illustrate this, the propose method is applied to the time rate of change of oxygen from the model after removing the contribution of the local flux divergence. This correction significantly reduces the bias associated with the vertical position near the sea surface (Figure 13).

While the analysis above demonstrates that the method can reasonably estimate the rate of GPP, the method is not accurate enough to provide an estimate of CR. In the simulations presented above, the divergence in vertical flux is the dominant contributor to $\Delta\widehat{O}_2$ and separating the contribution of CR is not possible with the proposed method. Even if the flux divergence were accurately known, the contributions of horizontal and vertical advection are still not insignificant compared to the relatively small difference between GPP and CR. Thus, estimating NEM in an estuarine environment like Chesapeake Bay using diel techniques is unlikely to yield accurate results. While the influence of horizontal advection is significantly reduced in lake environments, the issues associated with vertical mixing and uncertainties in the application of the surface flux correction are likely to introduce significant environments in these environments as well.

6. Conclusions

In this paper, a relatively simple diel method to estimate GPP and the underlying *PE* curve parameters is presented and tested against a numerical circulation model with a realistic representation of biological oxygen dynamics. The method relies on the statistical relationship between the time rate of change of near-surface oxygen concentration and incoming solar radiation. Evaluation of the method applied at a depth of $z \sim -1$ m demonstrates that GPP can be estimated with significant skill even when in situ observations of PAR are not available. In order to avoid potential biases due to advection, the method is best applied over a 15-day period in order to minimize the correlation between semidiurnal (tidal) and diurnal (solar) processes. The primary source of bias comes from diurnal contributions from the divergence in vertical oxygen flux, which are minimized at some optimal location within the euphotic zone. Above this location, estimates of GPP are underpredicted, and below this location, estimates are overpredicted, largely due to the contributions of vertical mixing. Errors are enhanced when GPP varies strongly in the vertical and for conditions when the surface mixed layer is deeper than the euphotic depth. Proposed methods that "correct" the time rate of change of oxygen using estimates of the flux divergence based on the atmospheric gas flux are unlikely to be effective for measurements collected at a fixed vertical location given the structure of the flux divergence near the surface. The proposed method shows significant promise for estimating GPP at a variety of time scales using oxygen data that are routinely collected through ocean observing systems.

Acknowledgments
This paper is the result of research funded in part by NOAA's U.S. Integrated Ocean Observing System (IOOS) Program Office as a subcontract to the Woods Hole Oceanographic Institution under award NA13NOS120139 to the Southeastern University Research Association. All of the model output, as well as both the CBIBS data (2010–2016) and the bottom oxygen data of Scully (2016b), are publicly available through the THREDDS server associated with the IOOS Coastal Modeling Testbed site: https://comt.ioos.us/projects/cb_hypoxia.

References

Beck, M. W., Hagy, J., & Murrell, M. (2015). Improving estimates of ecosystem metabolism by reducing effects of tidal advection on dissolved oxygen time series. *Limnology and Oceanography: Methods*, *13*(12), 731–745. https://doi.org/10.1002/lom3.10062

Behrenfeld, M. J., Prasil, O., Babin, M., & Bruyant, F. (2004). In search of a physiological basis for covariations in light-limited and light-saturated photosynthesis. *Journal of Phycology*, *40*(1), 4–25. https://doi.org/10.1046/j.1529-8817.2004.03083.x

Bender, M., Grande, K., Johnson, K., Marra, J., Williams, P. J. L., Sieburth, J., et al. (1987). A comparison of four methods for determining planktonic community production. *Limnology and Oceanography*, *32*(5), 1085–1098. https://doi.org/10.4319/lo.1987.32.5.1085

Cloern, J. E., Grenz, C., & Vidergar-Lucas, L. (1995). An empirical model of the phytoplankton chlorophyll : carbon ratio—The conversion factor between productivity and growth rate. *Limnology and Oceanography*, *40*(7), 1313–1321. https://doi.org/10.4319/lo.1995.40.7.1313

Cole, J. J., Caraco, N. F., & Peierls, B. L. (1992). Can phytoplankton maintain a positive carbon balance in a turbid, freshwater, tidal estuary? *Limnology and Oceanography*, *37*(8), 1608–1617. https://doi.org/10.4319/lo.1992.37.8.1608

Cole, J. J., Pace, M. L., Carpenter, S. R., & Kitchell, J. F. (2000). Persistence of net heterotrophy in lakes during nutrient addition and food web manipulations. *Limnology and Oceanography*, *45*(8), 1718–1730. https://doi.org/10.4319/lo.2000.45.8.1718

Coloso, J. J., Cole, J. J., Hanson, P. C., & Pace, M. L. (2008). Depth-integrated, continuous estimates of metabolism in a clear-water lake. *Canadian Journal of Fisheries and Aquatic Sciences*, *65*(4), 712–722. https://doi.org/10.1139/f08-006

Cox, T. J., Maris, T., Soetaert, K., Kromkamp, J. C., Meire, P., & Meysman, F. (2015). Estimating primary production from oxygen time series: A novel approach in the frequency domain. *Limnology and Oceanography: Methods*, *13*(10), 529–552.

Falkowski, P. G., & Wirick, C. D. (1981). A simulation model of the effects of vertical mixing on primary productivity. *Marine Biology*, *65*(1), 69–75. https://doi.org/10.1007/BF00397069

Feng, Y., Friedrichs, M. A., Wilkin, J., Tian, H., Yang, Q., Hofmann, E. E., et al. (2015). Chesapeake Bay nitrogen fluxes derived from a land-estuarine ocean biogeochemical modeling system: Model description, evaluation, and nitrogen budgets. *Journal of Geophysical Research: Biogeosciences*, *120*, 1666–1695. https://doi.org/10.1002/2015JG002931

Fennel, K., Wilkin, J., Levin, J., Moisan, J., O'Reilly, J., & Haidvogel, D. (2006). Nitrogen cycling in the Middle Atlantic Bight: Results from a three-dimensional model and implications for the North Atlantic nitrogen budget. *Global Biogeochemical Cycles*, *20*, GB3007. https://doi.org/10.1029/2005GB002456

Gallegos, C. L. (2012). Phytoplankton photosynthetic capacity in a shallow estuary: Environmental correlates and interannual variation. *Marine Ecology Progress Series*, *463*, 23–37. https://doi.org/10.3354/meps09850

Harding, L. W. Jr., Meeson, B. W., & Fisher, T. R. Jr. (1986). Phytoplankton production in two east coast estuaries: Photosynthesis-light functions and patterns of carbon assimilation in Chesapeake and Delaware Bays. *Estuarine, Coastal and Shelf Science*, *23*(6), 773–806. https://doi.org/10.1016/0272-7714(86)90074-0

Howarth, R. W., Marino, R., Garritt, R., & Sherman, D. (1992). Ecosystem respiration and organic carbon processing in a large, tidally influenced river: The Hudson River. *Biogeochemistry*, *16*(2), 83–102.

Howarth, R. W., Schneider, R., & Swaney, D. (1996). Metabolism and organic carbon fluxes in the tidal freshwater Hudson River. *Estuaries*, *19*(4), 848–865. https://doi.org/10.2307/1352302

Irby, I. D., Friedrichs, M. A. M., Friedrichs, C. T., Bever, A. J., Hood, R. R., Lanerolle, L. W. J., et al. (2016). Challenges associated with modeling low-oxygen waters in Chesapeake Bay: A multiple model comparison. *Biogeosciences*, *13*(7), 2011–2028. https://doi.org/10.5194/bg-13-2011-2016

Jassby, A. D., & Platt, T. (1976). Mathematical formulation of the relationship between photosynthesis and light for phytoplankton. *Limnology and Oceanography*, *21*(4), 540–547. https://doi.org/10.4319/lo.1976.21.4.0540

Kantha, L. H., & Clayson, C. A. (1994). An improved mixed layer model for geophysical applications. *Journal of Geophysical Research*, *99*(C12), 25,235–25,266. https://doi.org/10.1029/94JC02257

Kemp, W. M., & Boynton, W. R. (1980). Influence of biological and physical processes on dissolved oxygen dynamics in an estuarine system: Implications for measurement of community metabolism. *Estuarine and Coastal Marine Science*, *11*(4), 407–431. https://doi.org/10.1016/S0302-3524(80)80065-X

Kirk, J. T. O. (1994). *Light and photosynthesis in aquatic ecosystems* (2nd ed.). Cambridge, MD: Cambridge University Press. https://doi.org/10.1017/CBO9780511623370

Laws, E. A. (1991). Photosynthetic quotients, new production and net community production in the open ocean. *Deep Sea Research Part A. Oceanographic Research Papers*, *38*(1), 143–167. https://doi.org/10.1016/0198-0149(91)90059-O

Lewis, M. R., Cullen, J. J., & Plantt, T. (1984). Relationships between vertical mixing and photoadaptation of phytoplankton: Similarity criteria. *Marine Ecology Progress Series*, *15*, 141–149. https://doi.org/10.3354/meps015141

Lewis, W. M. (1988). Primary production in the Orinoco River. *Ecology*, *69*(3), 679–692. https://doi.org/10.2307/1941016

Long, M. H., & Nicholson, D. P. (2017). Surface gas exchange determined from an aquatic eddy covariance floating platform. *Limnology and Oceanography: Methods* https://doi.org/10.1002/lom3.10233, *16*(3), 145–159.

MacIntyre, H. L., Kana, T. M., Anning, T., & Geider, R. J. (2002). Photoacclimation of photosynthesis irradiance response curves and photosynthetic pigments in microalgae and cyanobacteria. *Journal of Phycology*, *38*(1), 17–38. https://doi.org/10.1046/j.1529-8817.2002.00094.x

Malone, T. C., Conley, D. J., Fisher, T. R., Glibert, P. M., Harding, L. W., & Sellner, K. G. (1996). Scales of nutrient-limited phytoplankton productivity in Chesapeake Bay. *Estuaries*, *19*(2), 371–385. https://doi.org/10.2307/1352457

Marra, J. (2009). Net and gross productivity: Weighing in with ^{14}C. *Aquatic Microbial Ecology*, *56*, 123–131. https://doi.org/10.3354/ame01306

Milligan, A. J., Halsey, K. H., & Behrenfeld, M. J. (2015). Advancing interpretations of ^{14}C-uptake measurements in the context of phytoplankton physiology and ecology. *Journal of Plankton Research*, *37*(4), 692–698. https://doi.org/10.1093/plankt/fbv051

Odum, H. T. (1956). Primary production in flowing waters. *Limnology and Oceanography*, *1*(2), 102–117. https://doi.org/10.4319/lo.1956.1.2.0102

Peterson, B. J. (1980). Aquatic primary productivity and the ^{14}C-CO_2 method: A history of the productivity problem. *Annual Review of Ecology and Systematics*, *11*(1), 359–385. https://doi.org/10.1146/annurev.es.11.110180.002043

Richey, J. E., Devol, A. H., Hedges, J. I., Forsber, B., Victoria, R., Martinellis, L., & Ribeiro, N. (1990). Distributions and flux of carbon in the Amazon River. *Limnology and Oceanography*, *35*(2), 352–371. https://doi.org/10.4319/lo.1990.35.2.0352

Sargent, M. C., & Austin, T. S. (1949). Organic productivity of an atoll. *Eos, Transactions American Geophysical Union*, *30*(2), 245–249. https://doi.org/10.1029/TR030i002p00245

Scully, M. E. (2013). Physical controls on hypoxia in Chesapeake Bay: A numerical modeling study. *Journal of Geophysical Research: Oceans*, *118*, 1239–1256. https://doi.org/10.1002/jgrc.20138

Scully, M. E. (2016a). The contribution of physical processes to inter-annual variations of hypoxia in Chesapeake Bay: A 30-year modeling study. *Limnology and Oceanography*, *61*(6), 2243–2260. https://doi.org/10.1002/lno.10372

Scully, M. E. (2016b). Bathymetrically controlled mixing of dissolved oxygen in Chesapeake Bay. *Journal of Geophysical Research: Oceans*, *121*, 5639–5654. https://doi.org/10.1002/2016JC011924

Scully, M. E. (2018). A diel method of estimating gross primary production: 2. Application to 7 years of near-surface dissolved oxygen data in Chesapeake Bay. *Journal of Geophysical Research: Oceans*, *123*. https://doi.org/10.1029/2018JC014179

Staehr, P. A., Bade, D., Van de Bogert, M. C., Koch, G. R., Williamson, C., Hanson, P., et al. (2010). Lake metabolism and the diel oxygen technique: State of the science. *Limnology and Oceanography: Methods*, *8*(11), 628–644.

Staehr, P. A., & Sand-Jensen, K. (2007). Temporal dynamics and regulation of lake metabolism. *Limnology and Oceanography*, *52*(1), 108–120. https://doi.org/10.4319/lo.2007.52.1.0108

Staehr, P. A., Testa, J. M., Kemp, W. M., Cole, J. J., Sand-Jensen, K., & Smith, S. V. (2012). The metabolism of aquatic ecosystems: History, applications, and future challenges. *Aquatic Sciences*, *74*(1), 15–29. https://doi.org/10.1007/s00027-011-0199-2

Swaney, D. P., Howarth, R. W., & Butler, T. J. (1999). A novel approach for estimating ecosystem production and respiration in estuaries: Application to the oligohaline and mesohaline Hudson River. *Limnology and Oceanography*, *44*(6), 1509–1521. https://doi.org/10.4319/lo.1999.44.6.1509

Van de Bogert, M. C., Carpenter, S. R., Cole, J. J., & Pace, M. L. (2007). Assessing pelagic and benthic metabolism using free water measurements. *Limnology and Oceanography: Methods*, *5*(5), 145–155.

Wanninkhof, R. (2014). Relationship between wind speed and gas exchange over the ocean revisited. *Limnology and Oceanography: Methods*, *12*(6), 351–362.

Wilmott, C. J. (1981). On the validation of models. *Physical Geography*, *2*(2), 184–194. https://doi.org/10.1080/02723646.1981.10642213

Xu, J., Hood, R. R., & Chao, S. Y. (2005). A simple empirical optical model for simulating light attenuation variability in a partially mixed estuary. *Estuaries*, *28*(4), 572–580. https://doi.org/10.1007/BF02696068

Xu, J., Long, W., Wiggert, J. D., Lanerolle, L. W., Brown, C. W., Murtugudde, R., & Hood, R. R. (2012). Climate forcing and salinity variability in Chesapeake Bay, USA. *Estuaries and Coasts*, *35*(1), 237–261. https://doi.org/10.1007/s12237-011-9423-5